Meteoritics & Planetary Science 37, 229–244 (2002)
Available online at http://www.uark.edu/meteor

Fine-grained rims in the Allan Hills 81002 and Lewis Cliff 90500 CM2 meteorites: Their origin and modification

XIN HUA[1]*, JIANHUA WANG[2] AND PETER R. BUSECK[1,3]

[1]Department of Geological Sciences, Arizona State University, Box 871404, Tempe, Arizona 85287-1404, USA
[2]Department of Terrestrial Magnetism, the Carnegie Institution of Washington, 5241 Broad Branch Road Northwest, Washington D.C. 20015, USA
[3]Department of Chemistry/Biochemistry, Arizona State University, Box 871404, Tempe, Arizona 85287-1404, USA
*Correspondence author's e-mail address: huaxin@asu.edu

(Received 2000 August 7; accepted in revised form 2001 November 6)

Abstract–Antarctic CM meteorites Allan Hills (ALH) 81002 and Lewis Cliff (LEW) 90500 contain abundant fine-grained rims (FGRs) that surround a variety of coarse-grained objects. FGRs from both meteorites have similar compositions and petrographic features, independent of their enclosed objects. The FGRs are chemically homogeneous at the 10 μm scale for major and minor elements and at the 25 μm scale for trace elements. They display accretionary features and contain large amounts of volatiles, presumably water. They are depleted in Ca, Mn, and S but enriched in P. All FGRs show a slightly fractionated rare earth element (REE) pattern, with enrichments of Gd and Yb and depletion of Er. Gd is twice as abundant as Er.

Our results indicate that those FGRs are not genetically related to their enclosed cores. They were sampled from a reservoir of homogeneously mixed dust, prior to accretion to their parent body. The rim materials subsequently experienced aqueous alteration under identical conditions. Based on their mineral, textural, and especially chemical similarities, we conclude that ALH 81002 and LEW 90500 likely have a similar or identical source.

INTRODUCTION

Fine-grained materials occur as rims enclosing various coarse-grained objects in CM, CV, CO, OC3, and EC chondrites (Scott *et al.*, 1984; Rubin, 1984; MacPherson *et al.*, 1985; Rubin and Wasson, 1987; Metzler *et al.*, 1992; Zolensky *et al.*, 1993; Brearley, 1993, 1995; Alexander, 1995; Brearley *et al.*, 1995, 1999; Hua *et al.*, 1996; Tomeoka and Tanimura, 2000). They differ from the adjacent matrix by their grain sizes (<1 μm) and display features of both accretion of well-mixed dust grains and subsequent aqueous alteration. Their study is important for shedding light on the chemistry and accretionary history of chondritic materials in the early solar system. However, later processes such as aqueous alteration, brecciation, thermal metamorphism, and terrestrial weathering have removed much of the early record. Studies of the mineralogy of fine-grained rims (FGRs) are challenging because of their extremely fine-grained sizes.

We selected two Antarctic CM meteorites, Allan Hills (ALH) 81002 and Lewis Cliff (LEW) 90500, for our studies because both show well-preserved rims around almost all types of coarse-grained objects. The rims can reach several hundreds of micrometers in thickness, which is thick enough for a full characterization by different techniques at various magnifications. Hence we can obtain a comprehensive set of data for these special meteoritic components.

This paper reports the results of petrographic and chemical studies using scanning electron microscopy (SEM), electron microprobe analysis (EMPA), and secondary ion mass spectrometry (SIMS). The mineralogy of these FGRs using transmission electron microscopy (TEM) was reported in separate papers (Lauretta *et al.*, 2000; Hua *et al.*, unpubl. data).

SAMPLES AND ANALYTICAL METHODS

The same regions of two thin and polished sections of ALH 81002,30 and LEW 90500,60 were studied by optical microscopy, SEM, EMPA, and SIMS. Backscattered electron images (BSE) and chemical analyses were obtained with a JEOL JXA-8600 electron microprobe. Analyses were performed at a 15 kV accelerating voltage and 10 nA beam current using wavelength-dispersive x-ray spectroscopy (WDS). Counting times for both peak and background for each element was 30 s. The x-ray spatial resolution was ~2 μm for point analyses of individual mineral grains. FGRs were analyzed with a 10 μm defocused beam. A problem arises from defocused-beam analysis because there are small domains of different compositions in FGRs. These domains may introduce a

Prelude preprint MS#4416

systematic error in the corrected data, primarily from the fluorescence effect. However, since the FGRs have fairly uniform grain-size distributions and are compositionally homogeneous on the scale of 10 μm, EMPA can still produce useful information. For samples with grain sizes <1 μm, the average electron and x-ray paths may approximate those for homogeneous samples, and standard correction procedures are generally applicable (Albee *et al.*, 1977). Consequently, defocused-beam data can be reduced on-line using the empirical correction procedures of Albee and Ray (1970).

Standards included Amelia albite for Na, synthetic periclase (defocused beam) or natural enstatite (focused beam) for Mg, synthetic corundum (defocused beam) or Hakone anorthite (focused beam) for Al, Johnstown hypersthene for Si, Durango apatite for P, natural barite for S, OR-1 orthoclase for K, Yadkinville wollastonite for Ca, synthetic rutile for Ti, 52NL-11 chromite for Cr, Broken Hill rhodonite for Mn, synthetic wüstite (defocused beam) or synthetic fayalite (focused beam) for Fe, and synthetic NiO for Ni. The counts were corrected for dead time, background, and beam drift; matrix effects were corrected using Tracor-Northern ZAF matrix correction procedures. The detection limits for the analyzed elements are (in wt%) Na, Mg, Al, and Si = 0.01; P, Cr, and S = 0.03; K, Ca, and Ti = 0.02; Mn = 0.05, Fe = 0.07; and Ni = 0.08.

The trace elements were analyzed with a Cameca ims-6f ion probe at the Carnegie Institution of Washington, using a technique similar to that described by Zinner and Crozaz (1986). An O^- primary beam of ~2 nA at 12.5 kV was used and the spot size was ~25 μm. The secondary extraction voltage was set at 10 kV and an energy offset of –75 V with a 50 eV energy window was used to reduce molecular ion interference. Each measurement consisted of 100–200 cycles of peak jumping through selected masses. The electron multiplier background was <0.02 counts/s, monitored during all analyses at mass 130.5. The elemental concentrations were determined using reference elements Si (for silicates) and Ca (for carbonates), whose abundance were obtained from previous EMPA analysis. The analytical uncertainties are the standard errors in the mean abundance calculated from those of each cycle (Alexander, 1994).

OBSERVATIONS

Petrography

We checked 23 FGRs and their enclosed objects in a total area of ~1.6 cm^2 in ALH 81002 and ~1 cm^2 in LEW 90500 using optical microscopy and BSE imaging. FGRs are much more abundant than the inter-chondrule matrix (Figs. 1 and 2). Many show radial cracks extending between object–rim and rim–matrix interfaces. Both types of interfaces are well defined and sharp. All rims continuously surround their cores, similar to those of the Yamato (Y)-791198 CM chondrite (Metzler and Bischoff, 1989), indicating that ALH 81002 and LEW 90500 were not brecciated after FGR formation. The FGRs are texturally homogeneous and contain anhedral crystals of silicates, sulfides, and metal. Rim thickness differs from object to object and even from place to place around an individual object. The thickest parts reach several hundreds of micrometers at indented areas of some objects (double arrowheads in Figs. 1h and 2e). TEM observations on ALH 81002 and LEW 90500 reveal grains from 4 to 200 and 2 to 300 nm in size, respectively and show abundant aqueously altered phases and likely an amorphous material (Lauretta *et al.*, 1998, 2000; Li *et al.*, 1999).

The enclosed objects include (1) porphyritic olivine chondrules (both FeO-rich and FeO-poor; Figs. 1a,b and 2a,b,d,e,f,g); (2) barred olivine chondrules (both FeO-rich and FeO-poor; Fig. 2c); (3) microporphyritic olivine chondrules (FeO-poor; Fig. 1h); (4) individual olivine crystals (end-member forsterite, ~Fa_{50}, and zoned fayalitic olivines; Figs. 1d,e and 2d); (5) fayalitic olivine grains coexisting with apatite or phyllosilicates, or both (Fig. 1c,e); (6) PCP, a term originally defined by Fuchs *et al.* (1973) as p*oorly characterized phase* and later identified as an intergrowth of tochilinite and cronstedtite (Mackinnon and Zolensky, 1984; Tomeoka and Buseck, 1985) (Fig. 1f); (7) calcite crystals with outer tochilinite rinds (Fig. 2h); (8) calcite grains intergrown with spinel and titanofassaite (Fig. 1g, calcite was identified by its Raman spectrum); and (9) forsterite and tochilinite (Fig. 2i). The overall geometry, including FGR and core (FGR + C), is smooth and spherical to subspherical, which provides evidence that the (FGR + C) formed by the FGR materials filling into the embayed areas of cores and thinning at their prominences.

Major and Minor Element Chemistry

Bulk abundances of major (Si, Mg, S, Fe) and minor elements (Na, Al, P, K, Ca, Ti, Cr, Mn, and Ni) were determined for 91 spots from 15 FGRs using WDS with a 10 μm beam. Rims in both meteorites have very similar bulk compositions (Table 1, Fig. 3), although their enclosed cores differ greatly. FGRs are chemically homogeneous at the 10 μm scale of the EMPA beam, which is reflected by the small standard deviations from the mean values of all 13 measured elements. They are either below or close to 1%, except for Fe (3.16% for ALH 81002 and 2.44% for LEW 90500).

The FGRs display depletion of Ca, Mn, and S and enrichment of P. Calcium is significantly fractionated from Al: the Ca/Al ratios are 0.34 for FGRs in ALH 81002 and 0.31 for those in LEW 90500, which is well below the CI ratio of 1.09. This Ca depletion occurs even within the FGR that surrounds a core mainly consisting of calcite. In contrast to the other 14 CM meteorites (Fig. 4; Metzler *et al.*, 1992), the FGRs of our two CMs show a unique P enrichment but no Cr depletion. Except for Y-793321, Essebi, and Mighei, Metzler data show fractionation between Na and K, while our data do not show such fractionation. This discrepancy could be either real or a result of the different analytical and calibration

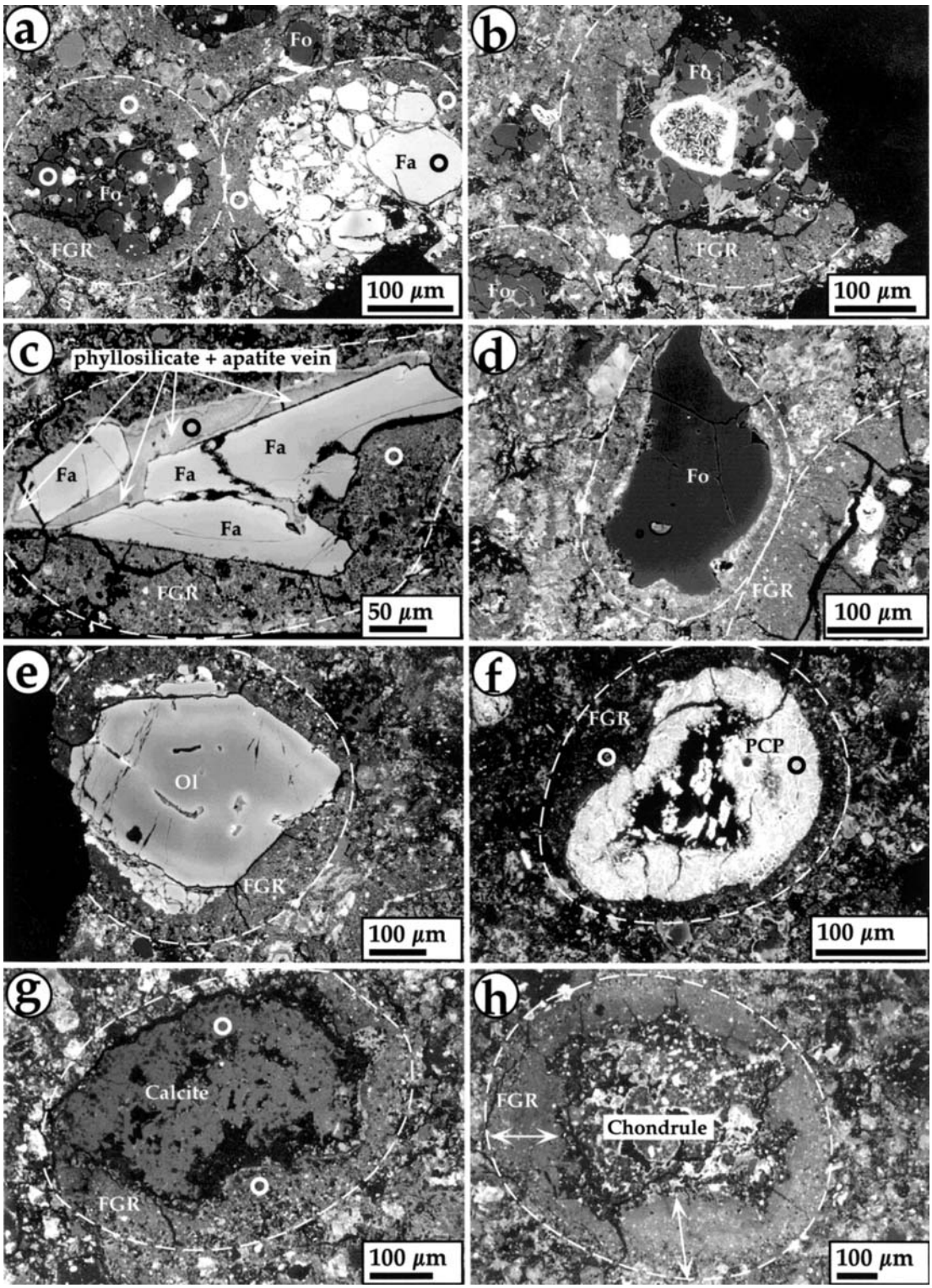

FIG. 1. Backscattered electron images of FGRs in LEW 90500 that surround (a) porphyritic forsteritic- and fayalitic-olivine chondrules; (b) porphyritic forsterite chondrules with a cluster of an intergrowth of tochilinite and cronstedtite in the middle of the chondrule; (c) several fayalitic olivine grains with veins of phyllosilicates and Ca-phosphates; (d) a forsterite crystal; (e) a zoned fayalitic olivine crystal; (f) an intergrowth of tochilinite and cronstedtite; (g) calcite intergrown with spinel and titanofassaite; and (h) a microporphyritic olivine chondrule. The dashed lines outline the FGRs on all coarse-grained objects, and the circles indicate the spots where the SIMS analyses were made. The double-headed arrows in (h) span the width of the FGR. Symbols used: Fo = forsterite, Fa = fayalite, FGR = fine-grained rim, Ol = olivine, PCP = an intergrowth of tochilinite and cronstedtite.

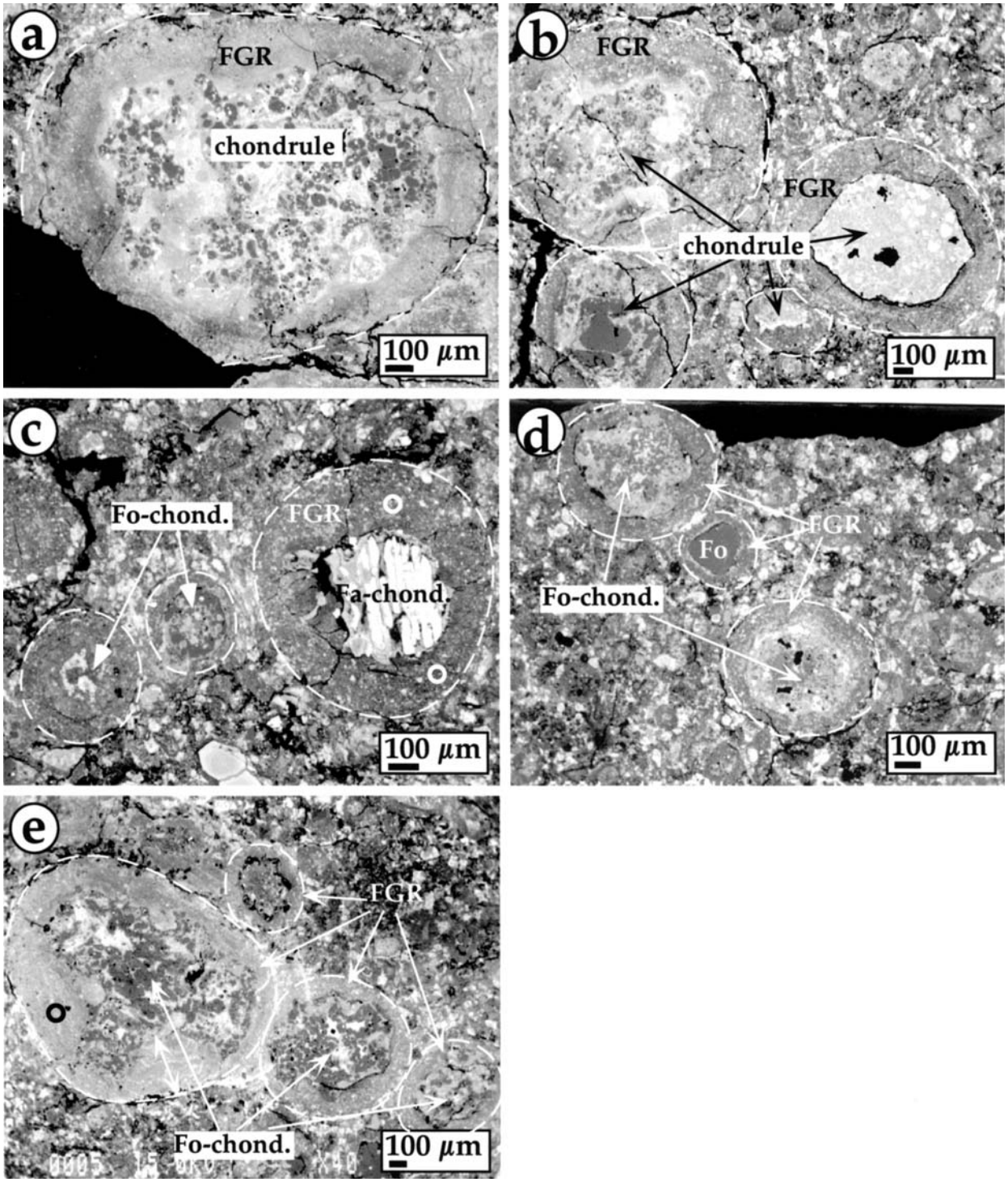

FIG. 2. Backscattered electron images of FGRs in ALH 81002 that surround (a) a porphyritic forsterite chondrule with a high proportion of anorthite glass; (b) four types of coarse-grained chondrules; (c) a barred fayalitic olivine chondrule and two porphyritic forsterite chondrules; (d) one porphyritic and one microporphyritic forsterite chondrule, and a single forsterite crystal; and (e) four porphyritic forsterite chondrules. The dashed lines outline the FGRs on all coarse-grained objects, and the circles indicate the spots where the SIMS analyses were made. The double-headed arrow in (e) spans the width of this FGR. Symbols used: FGR = fine-grained rim, Fo-chond. = forsterite chondrule, Fa-chond. = fayalite chondrule, Fo = forsterite, Tochili = tochilinite, Fo + Tochili = forsterite + tochilinite.

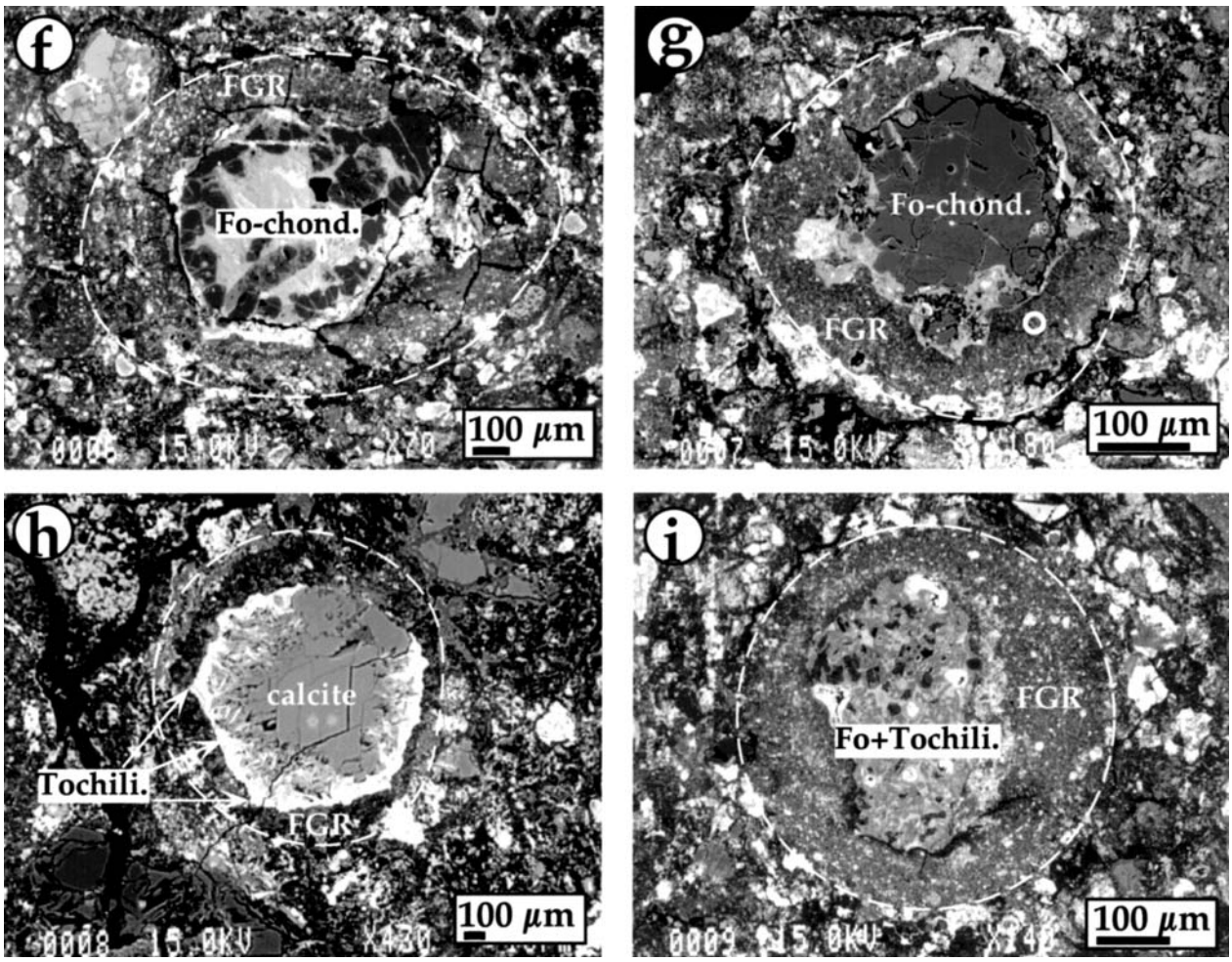

FIG. 2. *Continued.* Backscattered electron images of (f) a porphyritic forsterite chondrule with central anorthite glass; (g) a forsterite chondrule; (h) a calcite crystal with outer tochilinite rings; and (i) an aggregate of forsterite and tochilinite.

TABLE 1. Broad-beam EMPA analyses (wt%) of FGRs from ALH 81002 and LEW 90500.*

	ALH 81002				LEW 90500			
Number of analyses			45				46	
Na_2O	0.67	(0.15–1.54)	*0.4*	*(0.3)*	0.45	(0.20–2.00)	*0.4*	*(0.3)*
MgO	15.8	(12.2–18.4)	*1.4*	*(0.8)*	15.9	(12.0–19.8)	*1.4*	*(0.8)*
Al_2O_3	1.94	(1.38–2.93)	*0.3*	*(0.2)*	1.99	(1.80–3.02)	*0.3*	*(0.1)*
SiO_2	26.0	(17.1–30.1)	*2.7*	*(1.3)*	26.6	(23.1–30.8)	*1.9*	*(0.9)*
P_2O_5	0.31	(n.d.–1.28)	*0.3*	*(0.1)*	0.30	(n.d.–1.26)	*0.2*	*(0.1)*
SO_3	5.26	(2.40–11.6)	*1.7*	*(0.7)*	4.20	(1.82–6.72)	*0.2*	*(0.4)*
K_2O	0.08	(n. d.–0.19)	*0.04*	*(0.03)*	0.06	(n.d.–0.22)	*0.04*	*(0.04)*
CaO	0.49	(0.07–3.36)	*0.6*	*(0.4)*	0.44	(0.11–1.80)	*0.3*	*(0.2)*
TiO_2	0.07	(n. d.–0.15)	*0.03*	*(0.02)*	0.08	(0.05–0.18)	*0.03*	*(0.02)*
Cr_2O_3	0.50	(0.19–3.22)	*0.5*	*(0.4)*	0.40	(0.22–0.66)	*0.1*	*(0.1)*
MnO	0.18	(n.d.–0.65)	*0.09*	*(0.07)*	0.18	(n.d.–0.28)	*0.06*	*(0.04)*
FeO	22.8	(17.0–34.9)	*4.1*	*(3.2)*	24.3	(19.8–32.2)	*3.1*	*(2.4)*
NiO	1.76	(0.88–2.57)	*0.3*	*(0.3)*	1.59	(0.60–2.37)	*0.3*	*(0.2)*
Total	75.9	(56.3–84.4)	*4.9*		77.1	(72.7–84.6)	*2.7*	

*Numbers in parenthesis express compositional ranges. Numbers in italics express the standard deviations of oxides and elements (in parenthesis). n.d. = not detected.

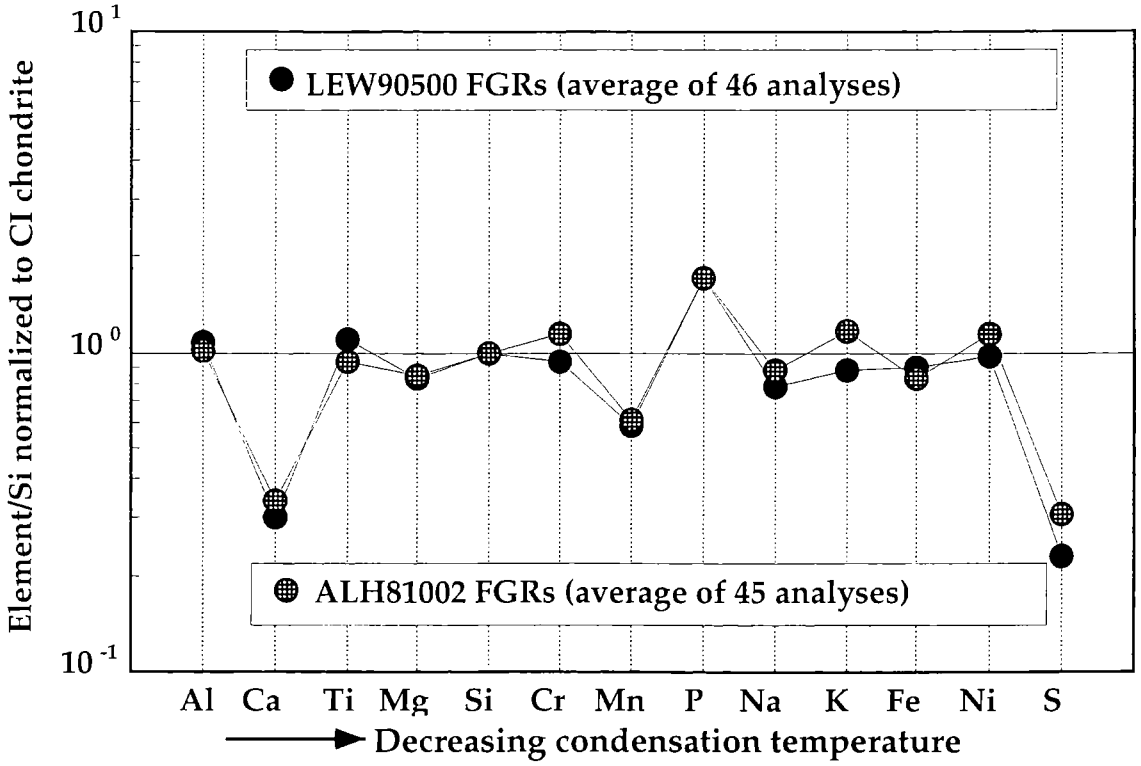

FIG. 3. Averages (wt%) from analyses at 91 spots of major and minor elements from FGRs around various coarse-grained objects from LEW 90500 and ALH 81002 chondrites. Concentrations are normalized to Si and CI chondritic compositions (Anders and Grevesse, 1989).

procedures used by different labs if we consider the volatile nature of Na during EPMA measurements.

The average totals of rim concentrations are 76 wt% for ALH 81002 and 77 wt% for LEW 90500 (Table 1). These low totals are presumably caused by the presence of water-bearing minerals and the porosity of the FGRs. The FGRs clearly show beam damage after EMPA analysis, which indicates the presence of volatiles, consistent with our TEM results (Lauretta *et al.*, 1998; Li *et al.*, 1999).

Individual analyses of FGRs are plotted onto a Fe-Mg-Si (wt% element) ternary diagram (Fig. 5). All data fall within a triangle that is defined by the compositions of PCP (a mixture of 25% tochilinite and 75% cronstedtite) and the compositional range of CM serpentines (McSween, 1987). The points lie close to a line from the Fe apex to the Si-Mg join, intercepting it at Mg/(Si + Mg) $\approx$ 0.45. This ratio is similar to that of other CM meteorites reported by Metzler *et al.* (1992) but smaller than the ratio of two FGRs from the Mokoia CV3 meteorite (Mg/(Si + Mg) $\approx$ 50) (Hua *et al.*, 1996) and larger than that of the ALHA77307 CO3 meteorite (Mg/(Si + Mg) $\approx$ 40) (Brearley, 1993). It is evident that the compositional variations of FGRs from these two meteorites follow the same trend as other CM meteorites, which show the same Si/Mg ratios but variable Fe contents. The variation in Fe contents can be interpreted as resulting from a heterogeneous distribution of metal and iron sulfides or from different proportions of PCP and Mg-rich serpentine within FGRs. Since PCP is rare within FGRs from these two meteorites (Lauretta *et al.*, 1998; Li *et al.*, 1999), the proportions of Mg-rich serpentine is key to understanding the extent of alteration. As pointed out by several workers (Tomeoka and Buseck, 1985; Tomeoka *et al.*, 1989; Browning *et al.*, 1996; Hanowski and Brearley, 2001) the Mg/Fe ratios of aqueously altered products increase proportionally to the intensity of aqueous alteration.

Trace Element Chemistry and Rare Earth Element Patterns

The abundances of 14 rare earth elements (REEs) and 15 other elements were measured using SIMS in three FGRs with four analyses spots in ALH 81002 (Table 2) and five FGRs with six analyses spots in LEW 90500 (Table 3). The major mineral constituents (*e.g.*, olivine, tochilinite, and calcite) of various rimmed objects and veins that occur among several fayalite grains (Fig. 1c) were also measured with SIMS but only from LEW 90500. We assume the same type of objects from both meteorites (Figs. 1 and 2) should have similar trace element concentrations. All analysis spots are marked as circles in Figs. 1 and 2. We did not list concentrations of Mg, Al, Si, Ca, and Fe in Tables 2 and 3 because SIMS data of these major elements are not as precise as those of EMPA, particularly when measuring the complex mixtures of minerals existing in fine-grained matrix and rims. The interaction volume between primary beam and

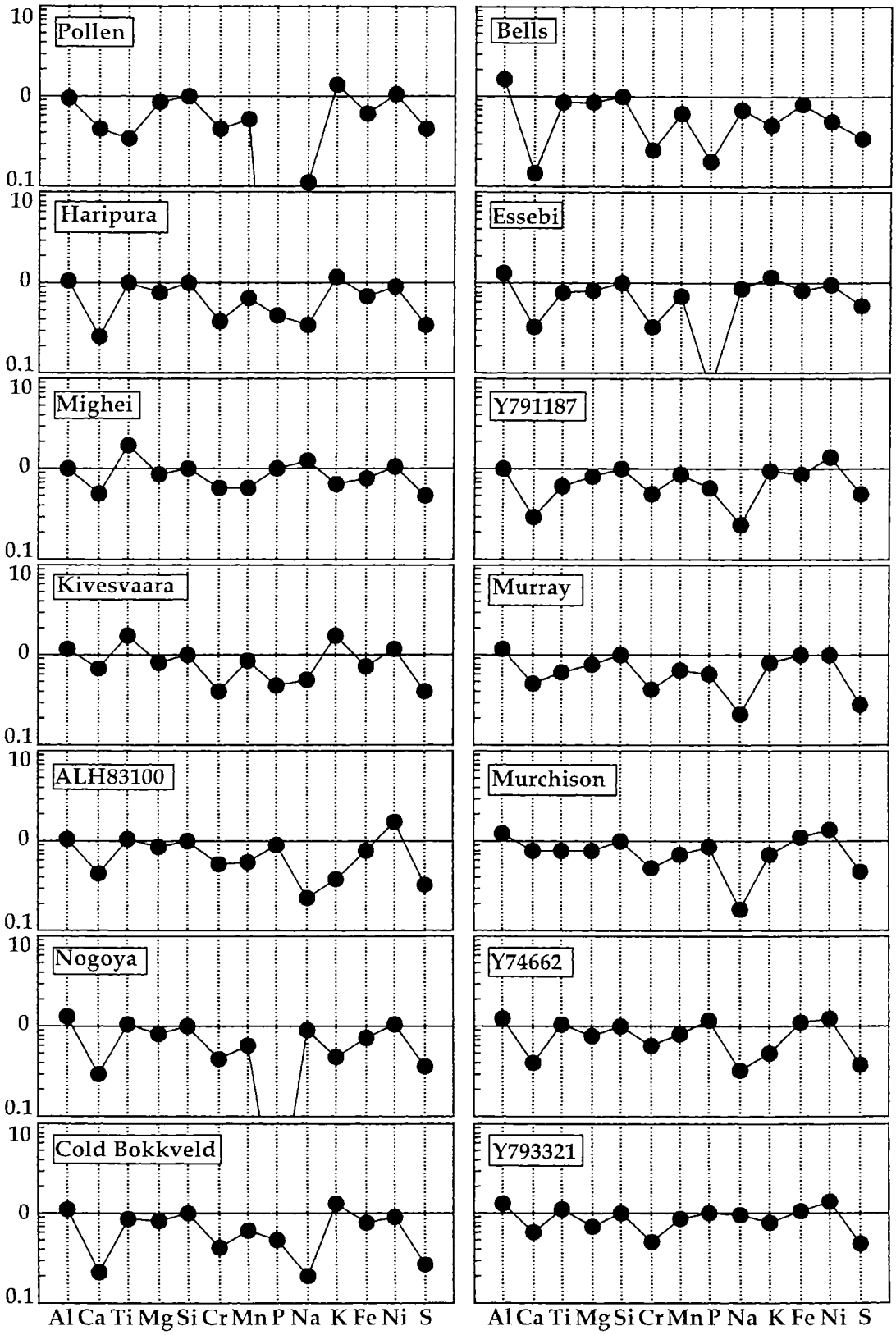

FIG. 4. Averaged concentrations (wt%) of major and minor elements of FGRs from CM chondrites, determined by defocused beam EMPA analyses (data are from Table 4 of Metzler *et al.*, 1992). Concentrations are normalized to Si and CI chondritic compositions.

TABLE 2. Concentrations of trace elements of ALH 81002 FGRs measured using the ion microprobe.*

	Fo		Fa	
	Rim-1	Rim-2	Rim-1	Rim-2
K	523	1340	1359	1210
Sc	43.7	22.7	14 ± 2.8	15 ± 2.6
Ti	1800 ± 212	657	732	740
Rb	4.58	3.9 ± 0.4	4.2 ± 1.8	17.7
Sr	18.7	6.50	23.2	25.8
Y	5.9 ± 0.63	1.73	2.84	3.49
Zr	12.0	8.7 ± 1.9	9.60	9.83
Nb	0.46	0.50	0.60	0.64
Ba	1.91	2.5 ± 0.28	5.15	6.44
La	1.08	0.18	0.51 ± 0.058	0.76
Ce	2.86	0.42	1.17	1.70
Pr	0.41	0.067 ± 0.008	0.18 ± 0.023	0.30
Nd	2.00	0.33	0.88	1.44
Sm	0.60	0.13 ± 0.014	0.31	0.42
Eu	0.14	0.048 ± 0.007	0.15	0.23
Gd	1.2 ± 0.13	0.25	0.56	0.92
Tb	0.17 ± 0.018	0.041 ± 0.005	0.087 ± 0.011	0.13
Dy	0.99	0.23	0.43	0.64
Ho	0.18	0.046 ± 0.006	0.071	0.11
Er	0.47	0.11	0.25	0.32
Tm	0.078	0.021 ± 0.003	0.037 ± 0.004	0.055
Yb	0.70	0.19	0.27	0.39
Lu	0.095	0.024	0.042	0.053

*All trace element concentrations are in ppm weight. Errors are given only if they exceed 10%.

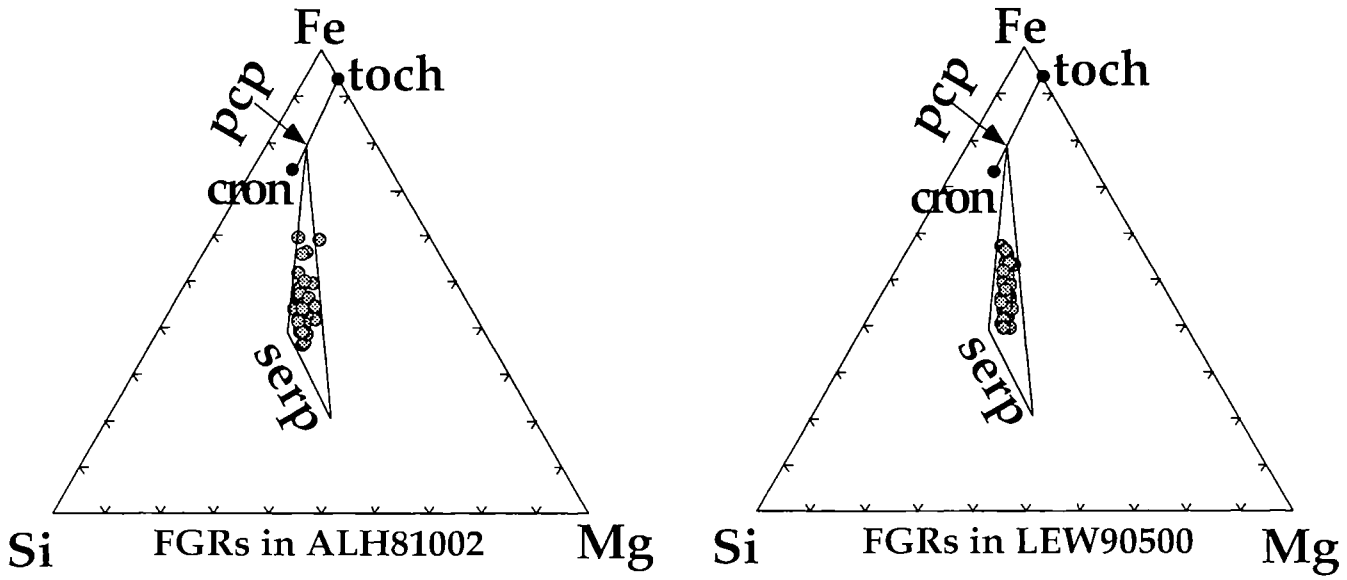

FIG. 5. Compositions (wt%) of individual EMPA analyses in FGRs from ALH 81002 and LEW 90500 chondrites, plotted in the ternary Fe-Si-Mg diagram. pcp = an intergrowth of tochilinite and cronstedtite; toch = tochilinite; cron = cronstedtite; serp = serpentine.

TABLE 3. Concentrations of trace elements measured using the ion microprobe (LEW 90500).*

	Ol chondrule				Calcite		PCP		Fa + Phyl + Ap	
	Fa-C	R-1	R-2	R-3	C	R	C	R	V	R
K	2.5 ± 1.1	1010	915	1215	56 ± 13	1157	6431	779	65.2	246 ± 38.5
Sc	8.1 ± 1.6	27 ± 2.7	14 ± 2.7	27.6	48.5	56.8	5.32	14 ± 1.8	10.8	5.9 ± 1.6
Ti	155	734	607	758	1003 ± 187	1553	470	670	597	302 ± 32.9
Rb	1.0 ± 0.15	5.4 ± 2.3	9.7 ± 1.6	5.9 ± 2.9	2.4 ± 0.9	9.75	32.5	4.3 ± 0.75	1.88	1.9 ± 1.5
Sr	0.15 ± 0.02	25.0	22.5	30.5	123 ± 13.2	17.93	103	18.2	6.38	6.3 ± 1.0
Y	0.13	3.12	3.31	3.30	28 ± 4.7	3.85	4.64	2.58	1.71	0.96 ± 0.16
Zr	0.067 ± 0.008	9.14	8.08	8.88	14.3	19.8	22.9	15 ± 2.9	5.62	2.6 ± 0.28
Nb	0.007 ± 0.002	0.55	0.47	0.59	1.5 ± 0.84	0.70	8.70	0.51	0.33	0.17 ± 0.02
Ba	0.066 ± 0.010	6.6 ± 0.7	7.10	8.15	32.7	4.36	45.8	4.78	1.27	1.8 ± 0.24
La	0.001 ± 0.001	0.60 ± 0.08	0.78	0.69	7.6 ± 0.97	0.62 ± 0.12	0.14	0.43	0.28	0.15 ± 0.02
Ce	0.003 ± 0.001	1.3 ± 0.15	1.76	1.55	18 ± 1.9	1.6 ± 0.26	0.17	1.07	0.70	0.37 ± 0.05
Pr	nd	0.22 ± 0.03	0.30	0.27	3.1 ± 0.65	0.26 ± 0.04	0.041 ± 0.005	0.19	0.12	0.062 ± 0.008
Nd	0.001 ± 0.001	1.02	1.45	1.40	14.6	1.16	0.43	0.90	0.63	0.31
Sm	0.002 ± 0.002	0.29	0.44	0.45	5.2 ± 0.78	0.37 ± 0.05	0.37 ± 0.048	0.27	0.20	0.070 ± 0.015
Eu	nd	0.18 ± 0.01	0.29	0.25	4.6 ± 1.6	0.16	0.25	0.14	0.076	0.049 ± 0.007
Gd	0.004 ± 0.001	0.64	1.07	1.00	16 ± 5.7	0.78	0.20	0.55	0.42	0.18 ± 0.018
Tb	nd	0.093	0.13	0.13 ± 0.02	2.3 ± 0.74	0.12	0.046	0.083	0.061	0.029 ± 0.004
Dy	0.009 ± 0.003	0.48	0.65	0.51	5.4 ± 0.78	0.69	0.054	0.35	0.26	0.15
Ho	0.005 ± 0.001	0.090	0.12	0.11 ± 0.013	0.98 ± 0.13	0.13	0.009 ± 0.002	0.069	0.058	0.027 ± 0.005
Er	0.008 ± 0.003	0.27	0.33	0.29	2.8 ± 0.33	0.43	0.059	0.25	0.18	0.079 ± 0.010
Tm	0.002 ± 0.001	0.039	0.054	0.058 ± 0.006	0.38 ± 0.078	0.056	0.030 ± 0.004	0.036	0.026	0.012 ± 0.003
Yb	0.033 ± 0.005	0.36	0.38	0.39	2.1 ± 0.47	0.51	0.070	0.28	0.21	0.11
Lu	0.006 ± 0.001	0.050	0.055	0.050 ± 0.005	0.40 ± 0.094	0.085	0.012 ± 0.002	0.037	0.031	0.016 ± 0.003

*All trace element concentrations are in ppm weight. Errors are given if they exceed 10%. nd = not detected. Abbreviations: C = core, R = rim, V = vein.

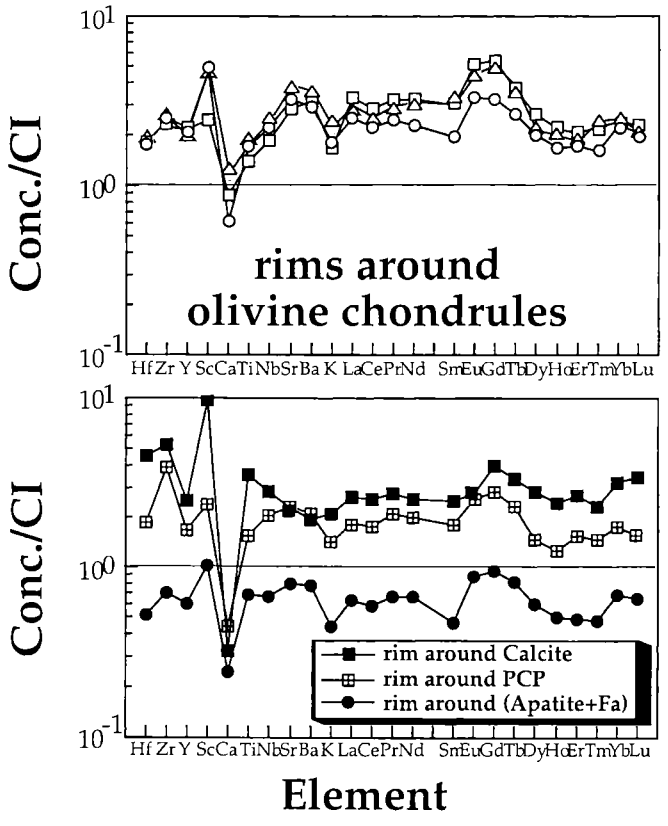

FIG. 6. REE and refractory element abundances for FGRs around several types of cores (LEW 90500). The upper plot shows the FGRs around olivine chondrules and the lower one shows FGRs around cores of calcite, an intergrowth of tochilinite and cronstedtite, and fayalite + apatite.

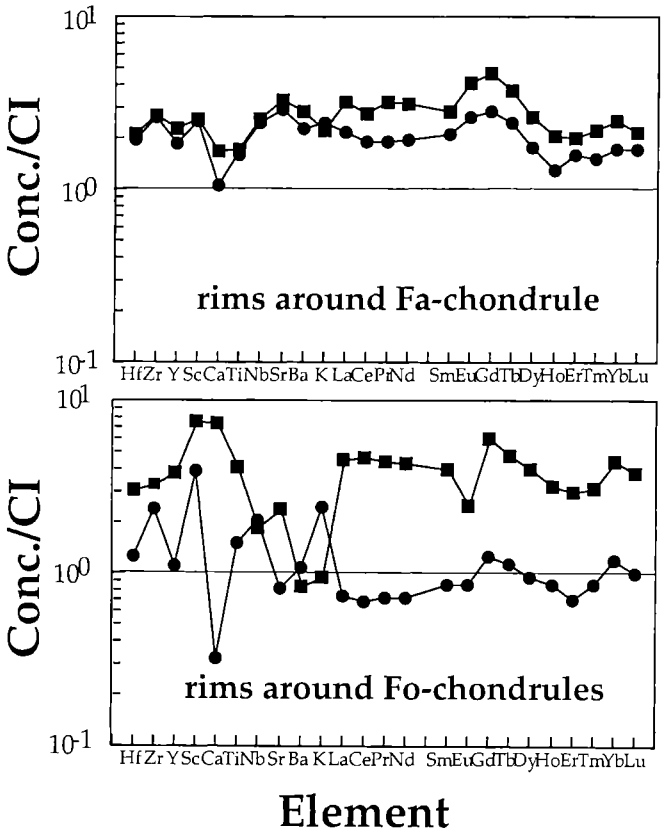

FIG. 7. REE and refractory element abundances for FGRs around fayalitic (upper) and forsteritic (lower) olivine chondrules (ALH 81002).

specimens in SIMS is much larger and deeper than that in EMPA. Therefore we used only EMPA data for major elemental concentrations and SIMS data for trace elemental concentrations.

CI-normalized abundance patterns of FGRs are displayed in Figs. 6 and 7. Nine of ten FGRs yield similar patterns of REE and other trace elements. Only one rim around a forsterite chondrule in ALH 81002 (Fig. 2e and the curve with solid squares in the lower part of Fig. 7) shows a different pattern; it displays higher Ca, Sr, and lower Eu than the other nine rims. This pattern probably resulted from large gypsum grains, whose existence within FGRs was confirmed by our TEM results (Lauretta *et al.*, 1998, 2000; Li *et al.*, 1999; Hua *et al.*, unpubl. data).

REE abundances vary by less than one order of magnitude from those of CIs. Eight of ten FGRs have higher concentrations than CIs. All FGRs have slightly fractionated REE patterns, with flat light rare earth elements (LREE), enrichment of Gd and Yb, and depletion of Er and the other heavy rare earth elements (HREE). Gadolinium is twice as abundant as Er. All FGRs but one show curves that go up from Sm to Gd, then gradually decline to Er and climb a little to Yb. Lutetium is lower than Yb in most analyses.

The trace element abundances of three core-minerals and their surrounding FGRs from LEW 90500 are plotted in Fig. 8a,c,d. The rims and core-minerals display significantly different abundances and distribution patterns in their trace elements. We did not measure the bulk REE compositions of the whole rimmed cores. Our data of cores are from single phases while data of FGRs are bulk; therefore this kind of comparison has some limitations. However, the minerals selected for SIMS analysis are the major phases, which occupy more than 95 vol% of individual cores. We therefore assume these minerals are the most important REE contributors to the cores. We also measured a vein containing phyllosilicates and apatite, which occurs within the grain boundaries of several fayalitic olivine crystals (Fig. 1c). In contrast to what has been mentioned above, the results show similar trace element patterns between the vein and its surrounding rim (Fig. 8b). This similarity indicates the FGR and vein may have experienced a similar aqueous alteration process on the meteorite parent body that modified their trace element chemistry.

DISCUSSION

It is necessary to consider the possibility of terrestrial weathering when analyzing Antarctic meteorites. Many workers

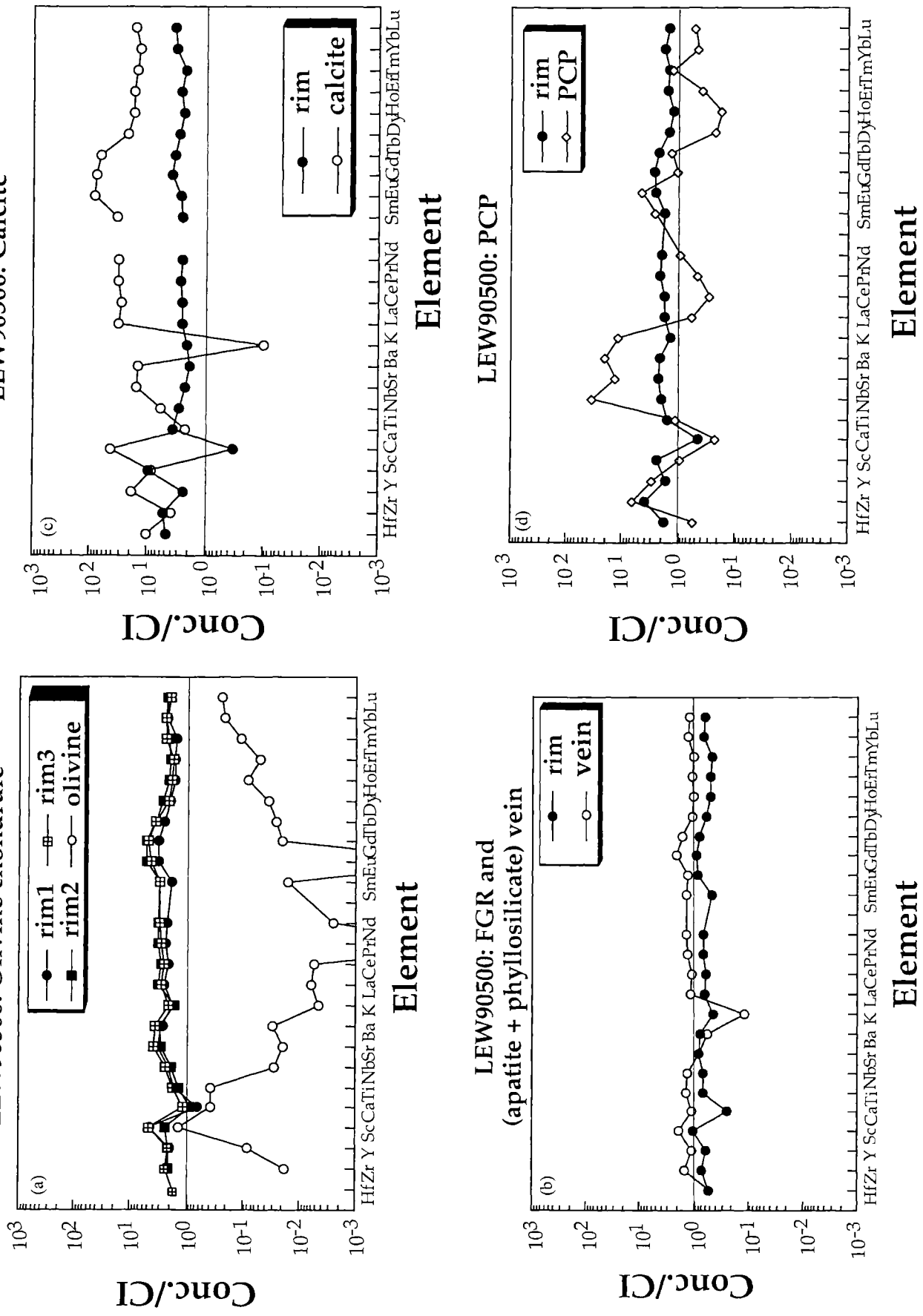

FIG. 8. REE and refractory element abundances for FGRs in LEW 90500 and the major mineral constituents of their enclosed cores or veins. Plots show (a) rims around olivine chondrules and olivine; (b) rim and a vein consisting of phyllosilicates and Ca phosphates; (c) rim and a mineral assemblage consisting mainly calcite, spinel, and titanofassaite; (d) rim and a cluster of an intergrowth of tochilinite and cronstedtite.

use the depletion of Na as an indicator of such weathering because Na is readily leached in the Antarctic environment. However, we did not observe significant Na depletion in ALH 81002 and LEW 90500 (Fig. 3); hence, we assume the terrestrial weathering of these two meteorites was limited and consider most features observed in our study as pre-terrestrial.

Several models have been proposed to explain the origin of FGRs in chondrites. The two extremes are: (1) FGRs formed in the solar nebula by accretion of well-mixed dust onto the surfaces of coarse-grained objects (Allen *et al.*, 1980; Bunch and Chang, 1980; King and King, 1981; Scott *et al.*, 1984; Rubin, 1984; MacPherson *et al.*, 1985; Rubin and Wasson, 1987; Brearley and Geiger, 1991; Tomeoka *et al.*, 1991; Nakamura *et al.*, 1991; Metzler *et al.*, 1992; Brearley, 1993; Hua *et al.*, 1996); and (2) FGRs formed in the regolith environment on the parent body(ies) by multiple stages of aqueous alteration and brecciation of the host chondrules (Sears *et al.*, 1993; Tomeoka and Tanimura, 2000). Other suggestions include shock melting from high-speed impact into regolith (Bunch *et al.*, 1991) and devitrification of chondrule melts (Hutchison and Bevan, 1983).

Based on our results from ALH 81002 and LEW 90500 we support the first model. Three important facts are emphasized in the following discussion: (1) the FGRs differ chemically and petrographically from their enclosed cores; (2) the FGRs contain fractionated patterns of REEs and the other trace elements that provide new insights to their origins; (3) the FGRs are remarkably similar in these two meteorites, suggesting they are genetically related.

Accretion of Fine-Grained Rims in the Solar Nebula

Although the mean compositions of individual FGRs in a given CM meteorite and among 14 different CM meteorites show systematically variations (Fig. 4; Metzler *et al.*, 1992), all our measured FGRs have similar major, minor, and trace element compositions (Figs. 3, 5, 6 and 7). Such similarities could have been produced by either sampling from the same sources or by an intensive regolith gardening on a meteorite parent body. Had FGRs formed by regolith gardening, their elemental composition should not only be the same from one rim to another but also be similar to the bulk composition of CM meteorites as a result of mixing of preexisting materials. However, our data show an obvious deviation from those of CMs, particularly in the abundances of Ca, Ti, P, Mn, K, and S (Fig. 9).

Nine out of ten FGRs from ALH 81002 and LEW 90500 yield similar patterns of REEs and other trace elements (Figs. 6 and 7), independent of their major core minerals (Fig. 8). Such similarities suggest that the same minerals host these trace elements, consistent with our major and minor elemental chemistry of FGRs. REE patterns of all FGRs are relatively flat and close to those of CIs, but their concentrations in individual rims can vary by less than one order of magnitude. Such variations indicate the heterogeneous distribution of trace-element carriers within FGRs, which is consistent with the mineral heterogeneity observed within the rims at the TEM scale (Lauretta *et al.*, 1998, 2000; Li *et al.*, 1999).

There is no physical evidence to support the regolith gardening. FGRs in ALH 81002 and LEW 90500 are remarkable homogeneous at the EMPA scale, and the grain sizes are <1 μm. If they formed in a regolith environment, the fragmentation of the precursor materials would have necessarily been very intensive. In that case, one would expect to find clasts that consist of fragments of different types of primary rocks and that are partly surrounded by FGRs, but there were not observed in these two meteorites. We observed FGRs completely surrounding all types of cores except at the edges of the thin sections (Figs. 1a,b,e and 2a,d), but none of these cores consist of polymict fragmented breccias. Radial cracks extend from core–rim interfaces through the FGRs but end at rim–matrix interfaces. It is difficult to imagine how these cracks could be restricted to FGRs through regolith gardening without extending into the adjacent matrix. The most likely explanation is that cracks in FGRs formed before the coarse-grained objects and their FGRs were embedded into the meteorite matrix.

Rim thicknesses vary from place to place around a given FGR, depending on the topography of their enclosed objects. They are thickest in the depressed parts and thin or absent at prominences of the coarse-grained objects. We interpret this rim morphology as an accretionary feature.

Modification of Fine-Grained Rims

All measured FGRs in ALH 81002 and LEW 90500 display depletion of Ca, Mn, and S, enrichment of P, and slightly fractionated patterns of REEs and the other trace elements. These features could have been produced in two ways. (1) The FGRs obtained their materials from the same dust reservoir that itself possessed the observed chemical characteristics. (2) The FGRs experienced subsequent processes that modified rim chemistry; such processes could have taken place in the nebula (such as evaporation, separation of preexisting dust from the vapor, and recondensation from the remaining vapor), or on intermediate bodies and/or simply on the meteorite parent body (through thermal metamorphism, brecciation, and aqueous alteration).

Fractionation of Ca from Al is common in essentially all fine-grained materials of chondrites (Metzler *et al.*, 1992; Brearley, 1993; Brearley *et al.*, 1995). The depletion of Ca in FGRs could be established in the nebula if FGRs were sampled from the remaining dust after the formation and isolation of calcium-aluminum-rich inclusions (CAIs). This hypothesis is consistent with the depletion of HREE in most of the FGRs (Figs. 6 and 7) because CAIs are known to remove most of the Ca and refractory HREEs. However this will cause a significant problem for chondrule formation, since chondrules formed several million years later than CAIs (Swindle *et al.*, 1996; Davis and MacPherson, 1996); if the above hypothesis is

correct, one should expect Ca depletion in chondrules too. However, for the most part chondrules have the solar Ca/Al ratio and unfractionated REEs.

An alternative process of Ca being decoupled from Al is aqueous alteration. Ca is much more soluble than Al and is readily transported in solution, whereas the mobility of Al is much less. The alteration of any Ca-Al-bearing minerals, whether it has a solar Ca/Al ratio or not, will result in the fractionation of Ca from Al. In that process Ca was transported away from the reacting mineral by a fluid and then precipitated elsewhere into secondary minerals such as phosphates, carbonates, and sulfates. This scenerio is confirmed by our EMPA data of the enrichment of P in FGRs (Fig. 3) and our TEM observation of the occurrence of these minerals in FGRs (Li *et al.*, 1999; Lauretta *et al.*, 2000; Hua *et al.*, unpubl. data). This mechanism is also demonstrated by the fact that veins formed by aqueous alteration in CI meteorites are filled with Mg and Ca carbonates and sulfates, although their bulk chemistry is depleted in Ca (Fredriksson and Kerridge, 1988). In addition, Brearley and Duke (1998) reported the results of their low-temperature hydrothermal experiments on Allende, in which calcium carbonates and sulfates were easily produced, an effective mechanism to fractionate Ca from Al. Since the bulk Ca/Al ratios of ALH 81002 and LEW 90500 are solar (Hanowski and Brearley, 2001) the Ca-depletion in FGRs must be produced by element exchange in a closed system. Such closed system processes are consistent with the aqueous alteration on meteorite parent body(ies).

Aqueous alteration has also played an important role in modifying the REE chemistry and mineralogy of FGRs. Chondrules from these two meteorites were observed to have experienced extensive alteration (Hanowski and Brearley, 2001). Rims essentially consist of much finer-grained materials than chondrules; hence they should have experienced highly advanced aqueous alteration. The low totals of average concentrations in FGRs (76 wt% for ALH 81002 and 77 wt% for LEW 90500) and the obvious beam damage shown on spots of FGRs after the EMPA analysis are consistent with the presence of water in FGR materials. Using TEM, we also identified serpentine, cronstedtite, tochilinite, pentlandite, ferrihydrite, and calcium sulfate (gypsum or anhydrite) within FGRs (Li *et al.*, 1999; Lauretta *et al.*, 2000; Hua *et al.*, unpubl. data). These minerals are products of aqueous processes (Bunch and Chang, 1980; Scott *et al.*, 1988; Zolensky and McSween, 1988; Tomeoka *et al.*, 1989; Buseck and Hua, 1993) and could contain information regarding the mobilization and redistribution of REEs.

All our measured FGRs show an enrichment of Eu, Gd, and Yb, and depletion of Er. Although such patterns are unusual, the possibility of analytical artifacts can be ruled out because no enrichment in HREE was observed. Artifacts can be generated by mass overlaps of oxide interference from LREE to middle rare earth elements (MREE), but such interference should also affect HREE (Shimizu, 1999; pers. comm.). Machine fractionation with an ion probe may change REE concentrations, but they will change all REEs to the same degree rather than produce fractionation among different REEs. Therefore, our measured patterns could not be generated by SIMS but are most likely original. Both post-accretionary aqueous alteration and preaccretionary condensation need to be considered to explain our REE data of FGRs.

Eight of ten rims we measured show higher REE concentrations than that of CIs (Figs. 6 and 7), which indicates a transport of REEs from somewhere into the rims. For instance, REEs could have been mobilized from chondrules into secondary minerals of rims during post-accretional aqueous alteration. This conclusion is based on the assumption that the original accretionary rim materials have unfractionated REEs as most chondritic matrices. We note that two papers described the advanced alteration of chondrule silicates from ALH 81002 and LEW 90500 (Hanowski and Brealey, 1997, 2001). The authors proposed a four-stage alteration sequence, in which mesostasis glass has been completely replaced by phyllosilicates during the first stage and clinopyroxene has been aqueously altered during the second stage. This alteration process is consistent with our REE data. Among chondrule silicates, clinopyroxene is one of the most important phases to take up the REEs from the melt of chondrule droplet and selectively enrich the melt in the LREE. If the mesostasis glass of chondrules completely reacted with a fluid, REEs, particularly LREE, would be transported from the glass into phyllosilicates, causing FGRs to be enriched in bulk REEs. Further alteration would cause the breakdown of clinopyroxene and would redistribute the REEs with a depletion of HREE. Conversely, olivine contains one to two orders of magnitude less REE than the other major silicates; very little or no change would be expected in the REE pattern during the alteration of olivine.

The above assessment can only provide limited information on the effects of secondary processes that change the REE chemistry. The primary minerals, the fluid, and the secondary products are the three major components that determine the variable REE chemistry by aqueous alteration. The physicochemical conditions in which the alteration takes place also play a crucial role in changing the REE chemistry. Furthermore, the ability of the newly formed minerals to accommodate the REE, either within their crystal structures or by adsorption, will be important factors in determining the bulk REE patterns of the altered sample. The proportion of certain types of minerals is also important. All these factors are not well known. We have to make some predictions, such as the possible primary minerals that would have broken down and released REE, the likelihood that secondary minerals could take up the REE, a fluid that might progressively change its chemistry during the trend of alteration, and the environmental conditions that prevailed during alteration.

The variations in volatility of REEs are large, ranging over a factor of 10^8 in the solar system (Boynton, 1975, 1988). The fractionated REE patterns of the FGRs could be also produced by

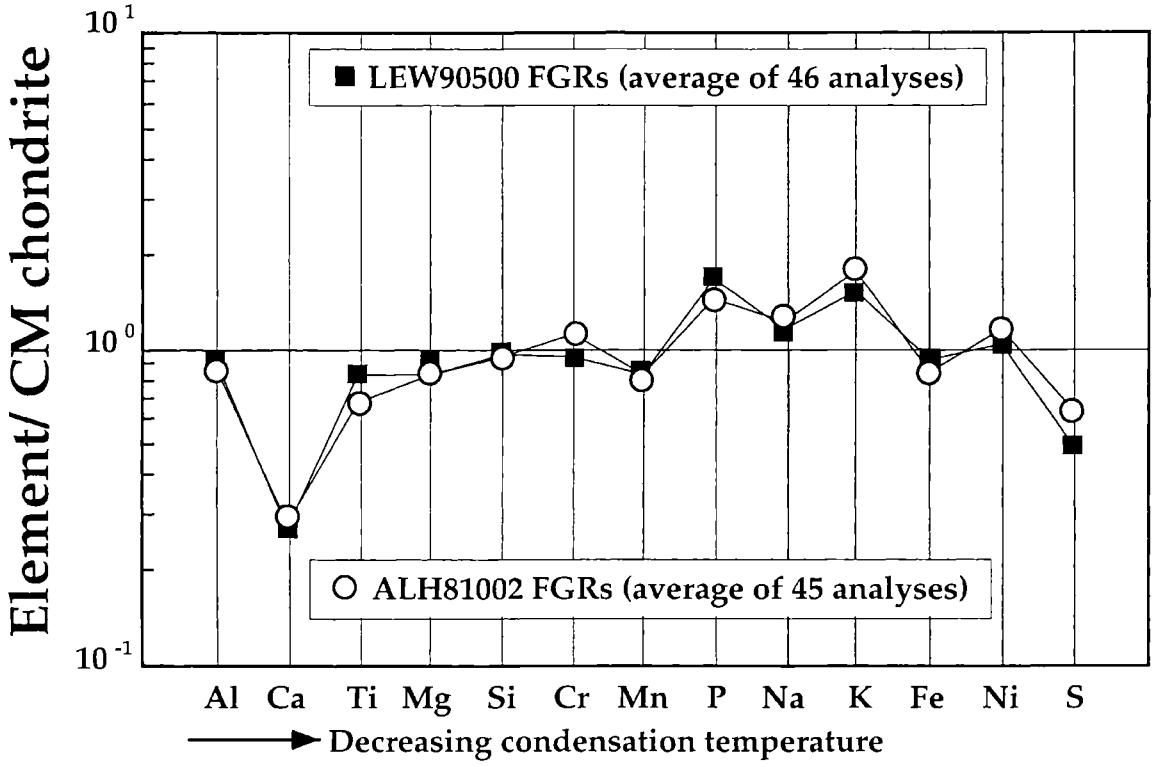

FIG. 9. Averaged concentrations (wt%) of major and minor elements from FGRs around various coarse-grained objects from LEW 90500 and ALH 81002 chondrites. Concentrations are normalized to CM chondritic compositions (Anders and Grevesse, 1989).

condensation or evaporation. At a total pressure of 10^{-3} atm, the condensation temperatures of pure REE sesquioxides are 1590 K for Er and 1140 K for Eu (Grossman and Ganapathy, 1976). The depletion of Er and enrichment of Eu, Gd, and Yb can be explained by sampling from the dust below 1590 K after the removal of Er and HREEs *via* refractory minerals such as perovskite, hibonite, and spinel. Under these conditions, the LREEs were not fractionated. Eu and Yb, although refractory, are among the most volatile REEs; hence, their enrichment suggests a relatively low-temperature origin. The positive Eu anomaly in the FGRs can be explained by condensation of the remaining gas after grains with the most REEs were removed from the nebula.

We believe that thermal metamorphism and brecciation were limited after the FGRs coated the coarse-grained objects in these two meteorites:

(1) If the meteorites had experienced intensive brecciation after FGR formation, one would expect to observe fragments containing different types of coarse-grained objects with a discontinuous FGR around each object. However, in the two meteorites we studied, FGRs occur at the outermost surfaces and completely surround almost all coarse-grained chondrules, CAIs, and mineral fragments and assemblages. They are much more abundant than the matrix. The rims are thicker than those in other chondrites. Therefore, significant brecciation to modify the FGRs in these two CM meteorites did not occur.

(2) FGRs could have experienced thermal metamorphism after they were incorporated into the meteorite parent body. However, the intensities of such metamorphism was low; otherwise, rims and chondrules would have been merged to produce new, larger chondrules, in which case no rims would have been preserved. This conclusion is consistent with the fact that rims are not as ubiquitous in more metamorphosed chondrites as those in CCs. Furthermore, the lack of evidence for equilibrated mineral assemblages within rims and the reaction between FGRs and either matrix or core precludes their having experienced intensive metamorphism.

(3) These two meteorites contain abundant organic materials that would not survive even mild metamorphism (Hanowski and Brearley, 2001). They also contain abundant hydrous phases and amorphous materials that would be unstable during mild thermal metamorphism.

Are they Paired Meteorites?

The compositions of FGRs in CCs normally differ from meteorite to meteorite, from rim to rim within the same meteorite, and even from layer to layer within the same rim (Metzler *et al.*, 1992; Hua *et al.*, 1996). In contrast, the FGRs in ALH 81002 and LEW 90500 are chemically identical and homogeneous. This uniformity suggests these two Antarctic meteorites are either paired or genetically related. If paired,

then this is the first pair collected from such widely separated locations (~875 km apart). However, based on the unpublished data of Nishiizumi (Nishiizumi *et al.*, 1993; pers. comm.), the exposure time is more than 3 Ma for ALH 81002 and ~0.6 Ma for LEW 90500; both meteorites have terrestrial ages shorter than 0.05 Ma. Therefore, pairing is unlikely.

CONCLUSIONS

(1) The FGRs in ALH 81002 and LEW 90500 are not genetically related to their enclosed cores; they formed before their meteorite parent body was accreted.

(2) These FGRs contain abundant altered materials with high contents of H_2O, which indicates that they have experienced highly aqueous alteration after they were embedded in the meteorite parent bodies .

(3) Rims in ALH 81002 and LEW 90500 have very similar compositions.

(4) In spite of their marked chemical and mineralogical similarities, ALH 81002 and LEW 90500 are not paired in their arrival on Earth, but they likely have a similar or identical source.

Acknowledgments—The ALH 81002 and LEW 90500 samples were provided by the NASA Meteorite Working Group. H. X. thanks the Carnegie Institution of Washington for hospitality during her visit there. We thank A. J. Brearley, L. Browning, and Ed Scott for their constructive and helpful reviews of the manuscript. We are grateful to Y. B. Guan, D. Lauretta, T. Zega, G. Huss, D. Jenney, and N. Shimizu for discussions. We thank J. Clark for assistance with electron microprobe analyses. This work was supported by NASA grant NAG5-4308 (P. R. B.).

Editorial handling: E. R. D. Scott

REFERENCES

ALBEE A. L. AND RAY L. (1970) Correction factors for electron probe microanalysis of silicate, oxides, carbonates, phosphates, and sulfates. *Anal. Chem.* **42**, 1408–1414.

ALBEE A. L., QUICK J. E. AND CHODOS A. A. (1977) Source and magnitude of errors in "broad-beam analyses" (DBA) with the electron probe (abstract). *Lunar Sci.* **8**, 7–9.

ALEXANDER C. M. O'D. (1994) Trace element distributions within ordinary chondrite chondrules: Implications for chondrule formation conditions and precursors. *Geochim. Cosmochim. Acta* **58**, 3451–3467.

ALEXANDER C. M. O'D. (1995) Trace element contents of chondrule rims and interchondrule matrix in ordinary chondrites. *Geochim. Cosmochim. Acta* **59**, 3247–3266.

ALLEN J. S., NOZETTE S. AND WILKENING L. L. (1980) A study of chondrule rims and chondrule irradiation records in unequilibrated ordinary chondrites. *Geochim. Cosmochim. Acta* **44**, 1161–1175.

ANDERS E. AND GREVESSE N. (1989) Abundances of the elements: Meteoritic and solar. *Geochim. Cosmochim. Acta* **53**, 197–214.

BOYNTON W. V. (1975) Fractionation in the solar nebula: Condensation of yttrium and the rare earth elements. *Geochim. Cosmochim. Acta* **39**, 569–584.

BOYNTON W. V. (1988) Nebular processes associated with CAI rim formation (abstract). *Meteoritics* **23**, 259.

BREARLEY A. J. (1993) Matrix and fine-grained rims in the unequilibrated CO3 chondrites, ALHA77307: Origins and evidence for diverse, primitive nebular dust components. *Geochim. Cosmochim. Acta* **57**, 1521–1550.

BREARLEY A. J. (1995) Aqueous alteration and brecciation in Bells, an unusual, saponite-bearing, CM chondrites. *Geochim. Cosmochim. Acta* **59**, 2291–2317.

BREARLEY A. AND DUKE C. L. (1998) Aqueous alteration of chondritic meteorites: Insights from experimental low temperature hydrothermal alteration of Allende (abstract). *Lunar Planet. Sci.* **29**, #1247, Lunar and Planetary Institute, Houston, Texas, USA (CD-ROM).

BREARLEY A. J. AND GEIGER T. (1991) Mineralogical and chemical studies bearing on the origin of accretionary rims in the Murchison CM2 carbonaceous chondrite (abstract). *Meteoritics* **26**, 323.

BREARLEY A. J., BAJT S. AND SUTTON S. R. (1995) Distribution of moderately volatile trace elements in fine-grained chondrule rims in the unequilibrated CO3 chondrite, ALHA77307. *Geochim. Cosmochim. Acta* **59**, 4307–4316.

BREARLEY A. J., HANOWSKI N. P. AND WHALEN J. F. (1999) Fine-grained rims in CM carbonaceous chondrites: A comparison of rims in Murchison and ALH81002 (abstract). *Lunar Planet. Sci.* **30**, #1460, Lunar and Planetary Institute, Houston, Texas, USA (CD-ROM).

BROWNING L. B., MCSWEEN H. Y., JR. AND ZOLENSKY M. (1996) Correlated alteration effects in CM carbonaceous chondrites. *Geochim. Cosmochim. Acta* **60**, 2621–2633.

BUNCH T. E. AND CHANG S. (1980) Carbonaceous chondrites—II. Carbonaceous chondrite phyllosilicates and light element geochemistry as indicators of parent body processes and surface conditions. *Geochim. Cosmochim. Acta* **44**, 1543–1578.

BUNCH T. E., CASSEN P., REYNOLDS R., CHANG S., PODOLAK M., PRIALNIK D. AND SCHULTZ P. H. (1991) Could chondrule rims be formed or modified by parent body accretion event? (abstract). *Meteoritics* **26**, 326.

BUSECK P. R. AND HUA X. (1993) Matrices of carbonaceous chondrite meteorites. *Ann. Rev. Earth Planet. Sci.* **21**, 255–305.

DAVIS M. A AND MACPHERSON G. J. (1996) Thermal processing in the solar nebular: Constraints from refractory inclusions. In *Chondrules and their Protoplanetary Disk* (eds. R. H. Hewins, R. H. Jones and E. R. D. Scott), pp. 71–76. Cambridge University Press, New York, New York, USA.

FREDRIKSSON K. AND KERRIDGE J. F. (1988) Carbonates and sulfates in CI chondrites: Formation by aqueous activity on the parent body. *Meteoritics* **23**, 35–44.

FUCHS L. H., OLSEN E. AND JENSEN K. J. (1973) Mineralogy, mineral-chemistry, and composition of the Murchison (C2) meteorite. *Smithson. Contrib. Earth Sci.* **10**, 1–39.

GROSSMAN L. AND GANAPATHY R. (1976) Trace elements in the Allende meteorite, I. Coarse-grained, Ca-rich inclusions. *Geochim. Cosmochim. Acta* **40**, 331–334.

HANOWSKI N. P. AND BREARLEY A. J. (1997) Transmission electron microscope observations of advanced silicate alteration in chondrules of the CM carbonaceous chondrite, Lewis Cliff 90500 (abstract). *Meteorit. Planet. Sci.* **32 (Suppl.)**, A56.

HANOWSKI N. P. AND BREARLEY A. J. (2001) Aqueous alteration of chondrules in the CM carbonaceous chondrite, Allan Hills 81002: Implications for parent body alteration. *Geochim. Cosmochim. Acta* **65**, 495–518.

HUA X., ZINNER E. K. AND BUSECK P. R. (1996) Petrography and chemistry of fine-grained dark rims in the Mokoia CV3 chondrite: Evidence for an accretionary origin. *Geochim. Cosmochim. Acta* **60**, 4265–4274.

HUTCHISON R. AND BEVAN A. W. R. (1983) Conditions and time of chondrule accretion. In *Chondrules and their Origins* (ed. E. A. King), pp. 162–179. Lunar and Planetary Institute, Houston, Texas, USA.

KING T. V. AND KING E. A. (1981) Accretionary dark rims in unequilibrated ordinary chondrites. *Icarus* **48**, 460–472.

LAURETTA D. S., HUA X. AND BUSECK P. R. (1998) Mineralogy of fine-grained rims in the Allan Hills 81002 CM carbonaceous chondrite determined by transmission electron microscopy (abstract). *Meteorit. Planet. Sci.* **33 (Suppl.)**, A91.

LAURETTA D. S., HUA X. AND BUSECK P. R. (2000) Mineralogy of fine-grained rims in the ALH 81002 CM chondrite. *Geochim. Cosmochim. Acta* **64**, 3263–3273.

LI J., HUA X., JANNEY D. E. AND BUSECK P. R. (1999) Mineralogy of a fine-grained rim in LEW90500 by transmission electron microscopy (abstract). *Lunar Planet. Sci.* **30**, #1271, Lunar and Planetary Institute, Houston, Texas, USA (CD-ROM).

MACKINNON I. D. R. AND ZOLENSKY M. (1984) Proposed structures for poorly characterized phases in C2M carbonaceous chondrite meteorites. *Nature* **309**, 240–242.

MACPHERSON G. J., HASHIMOTO A. AND GROSSMAN L. (1985) Accretionary rims on inclusions in the Allende meteorite. *Geochim. Cosmochim. Acta* **49**, 2267–2279.

MCSWEEN H. Y., JR. (1987) Aqueous alteration in carbonaceous chondrites: Mass balance constraints on matrix mineralogy. *Geochim. Cosmochim. Acta* **51**, 2469–2477.

METZLER K. AND BISCHOFF A. (1989) Accretionary dust mantles in CM chondrites as indicators for processes prior to parent body formation (abstract). *Lunar Planet. Sci.* **20**, 689–690.

METZLER K., BISCHOFF A. AND STÖFFLER D. (1992) Accretionary dust mantles in CM chondrites: Evidence for solar nebula processes. *Geochim. Cosmochim. Acta* **56**, 2873–2897.

NAKAMURA T., TOMEOKA K., AND TAKEDA H. (1991) Mineralogy of chondrule rims in the Yamato-79118 CM chondrite: Comparison to Murchison (abstract). *Symp. Antarc. Meteor.* **16th**, 40–41.

NISHIIZUMI K., ARNOLD J. R., CAFFEE M. W., FINKEL R. C., SOUTHON J. R., NAGAI H., HONDA M., IMAMURA M., KOBAYASHI K. AND SHARMA P. (1993) Exposure ages of carbonaceous chondrites—I (abstract). *Lunar Planet. Sci.* **24**, 1085–1086.

RUBIN A. E. (1984) Coarse-grained chondrule rims in type 3 chondrites. *Geochim. Cosmochim. Acta* **48**, 1779–1789.

RUBIN A. E. AND WASSON J. T. (1987) Chondrules, matrix, and coarse-grained chondrule rims in the Allende meteorite: Origin, interrelationships and possible precursor components. *Geochim. Cosmochim. Acta* **51**, 1923–1937.

SCOTT E. R. D., RUBIN A. E., TAYLOR G. J. AND KEIL K. (1984) Matrix material in type 3 chondrites—occurrence, heterogeneity and relationship with chondrules. *Geochim. Cosmochim. Acta* **48**, 1741–1757.

SCOTT E. R. D., BARBER D. J., ALEXANDER C. M. O'D., HUTCHISON R., AND PECK J. A. (1988) Primitive material surviving in chondrites: Matrix. In *Meteorites and the Early Solar System* (eds. J. F. Kerridge and M. S. Matthews), pp. 718–745. Univ. Arizona Press, Tucson, Arizona, USA.

SEARS D. W. G., BENOIT P. H. AND LU J. (1993) Two chondrule groups each with distinctive rims in Murchison recognized by cathodoluminescence. *Meteoritics* **28**, 669–675.

SWINDLE T. D., DAVIS A. M., HOHENBERG C. M., MACPHERSON G. J. AND NYQUIST L. E. (1996) Formation times of chondrules and Ca-Al-rich inclusions: Constraints from short-lived radionuclides. In *Chondrules and the Protoplanetary Disk* (eds. R. H. Hewins, R. H. Jones and E. R. D. Scott), pp. 77–86. Cambridge University Press, New York, New York, USA.

TOMEOKA K. AND BUSECK P. R. (1985) Indicators of aqueous alteration in CM carbonaceous chondrites: Microtextures of a layered mineral containing Fe, S, O and Ni. *Geochim. Cosmochim. Acta* **49**, 2149–2163.

TOMEOKA K. AND TANIMURA I. (2000) Phyllosilicate-rich chondrule rims in the Vigarano CV3 chondrite: Evidence for parent-body processes. *Geochim. Cosmochim. Acta* **64**, 1971–1988.

TOMEOKA K., MCSWEEN H. Y., JR. AND BUSECK P. R. (1989) Mineralogical alteration of CM carbonaceous chondrites: A review. *Proc. NIPR Symp. Antarct. Meteorites* **2**, 221–234.

TOMEOKA K., HATAKEYAMA K., NAKAMURA T. AND TAKEDA H. (1991) Evidence for pre-accretionary aqueous alteration in the Y-793321 CM carbonaceous chondrite (abstract). *Symp. Antarc. Meteor.* **16th**, 37–39.

ZINNER E. AND CROZAZ G. (1986) A method for the quantitative measurement of rare earth elements in the ion microprobe. *Intl. J. Mass Spectrom. Ion Processes* **69**, 17–38.

ZOLENSKY M. AND MCSWEEN H. Y., JR. (1988) Aqueous alteration. In *Meteorites and the Early Solar System* (eds. J. F. Kerridge and M. S. Matthews), pp. 114–143. Univ. Arizona Press, Tucson, Arizona, USA.

ZOLENSKY M., BARRETT R. AND BROWNING L. (1993) Mineralogy and composition of matrix and chondrule rims in carbonaceous chondrites. *Geochim. Cosmochim. Acta* **57**, 3123–3148.